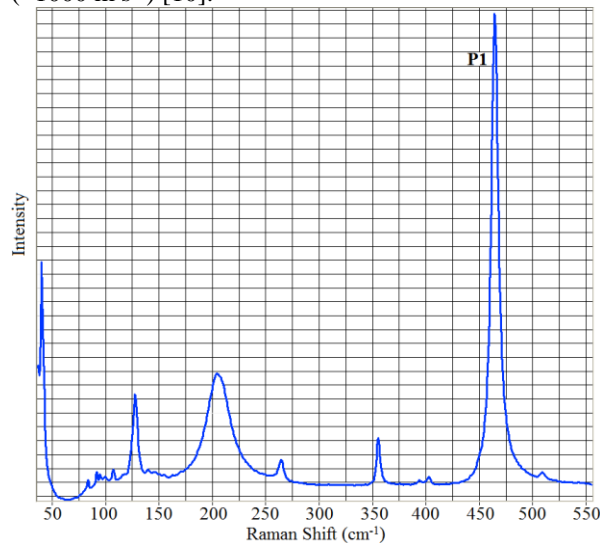


**THE EFFECTS OF SHOCK PRESSURE ON THE RAMAN SPECTRUM OF HIGH PURITY QUARTZ CRYSTALS.** R. Hibbert<sup>1</sup>, M. C. Price<sup>1</sup>, T. M. Kinnear<sup>1</sup>, M. J. Cole<sup>1</sup> and M. J. Burchell<sup>1</sup>, <sup>1</sup>Centre for Astrophysics and Planetary Science, School of Physical Sciences, Univ. of Kent, Canterbury, CT2 7NH. (E-mail: rh443@kent.ac.uk).

**Introduction:** Quartz ( $\text{SiO}_2$ ) is known to be present on Mars and has been identified in its crystalline form near Antoniadi Crater on the northern edge of the Syrtis Major shield volcano [1]. The *ExoMars* rover, due to launch in 2018, will be the first Raman spectrometer deployed on another planetary body [2, 3]. Impacts occur throughout the solar system, including the Martian surface, where they can hit terrains in excess of three billion years old. Work at the University of Kent has shown the shock effects of such impacts result in the modification of minerals and organics [4, 5] and can include a loss of volatiles [6, 7, 8]. This study aims to investigate how shock effects alter the Raman spectrum of quartz.

**Methodology:** The University of Kent's two stage light gas gun (LGG) [9] can fire either a single projectile of up to 3 mm diameter or a buckshot of smaller sized material at speeds between 1.1 and 8.0  $\text{km s}^{-1}$ , which can be measured to an accuracy of 1%. Recently, we have developed the capability of firing at speeds lower than 1  $\text{km s}^{-1}$ . This was done by modifying the gun to work as a single stage light gas gun. The aluminium burst disk is replaced with either a 250  $\mu\text{m}$  thick Mylar disk or 50  $\mu\text{m}$  thick aluminium foil. Varying speeds are achieved by changing the gas in the pump tube:  $\text{N}_2$  ( $\sim 380 \text{ m s}^{-1}$ ), He ( $\sim 600 \text{ m s}^{-1}$ ),  $\text{H}_2$  ( $\sim 1000 \text{ m s}^{-1}$ ) [10].



**Fig. 1:** Raman spectrum of quartz at 25°C with the main peak at  $464 \text{ cm}^{-1}$  labelled as 'P1'.

Raman spectroscopy uses monochromatic laser light to illuminate a sample. When the laser light

strikes a molecule in the sample, most of the light is unaffected and can be detected at its original wavelength. A very small amount of the light, however, shifts due to interaction with the molecule and can be detected at wavelengths specific to the composition of the sample. This is known as Raman scattering. Because the Raman scattering is specific to the composition of the sample, Raman spectroscopy can be used to identify specific molecular bonds within the sample.

The University of Kent's Raman spectrometer is a Horiba LabRam-HR which can use four lasers: near infrared (785 nm), red (633 nm), green (532 nm), and blue (473 nm). The work carried out in this investigation used the 532 nm laser that mimics the laser which will be carried on *ExoMars*. The Raman spectrum for unshocked quartz at 25°C is presented in Fig. 1, with the main peak, located at  $464 \text{ cm}^{-1}$ , labelled 'P1'.

**Method:** A buckshot of 50  $\mu\text{m}$  diameter molybdenum spheres were impacted into a target consisting of a 9.03 ct, 12 mm by 16 mm, quartz gem at a range of speeds (0.910 – 5.27  $\text{km s}^{-1}$ ). Raman maps of these quartz gemstones were then taken and analysed using a Python script. The Python script used the least squares method to fit curves to the P1 peak of each of the spectra in the map. The peak position of these fits was then recorded and compared to the unshocked position of the peak. This then allows for the production of a 2D map of the crater displaying the amount of peak shift due to the shock pressures induced by the impact at each point on the map.

**Results:** The slowest speed shot presented here is 0.910  $\text{km s}^{-1}$ , which did not generate a crater in the surface of the quartz gemstone, but rather left a small impression or 'bruise' in the surface (Fig. 2a). The Raman shift map of this 'bruise' shows that while there are regions of small positive shift in the P1 position, the central area of the 'bruise' largely consists of negative shift, reaching a maximum of  $-1.46 \text{ cm}^{-1}$  (Fig. 2b).

Further shots were conducted at a range of speeds up to 5.27  $\text{km s}^{-1}$  (Table 1). These faster shots all produced craters in the surface of the quartz gemstone and all showed positive shifts in the P1 position. The slowest shot that produced a crater was at 1.35  $\text{km s}^{-1}$  and showed a maximum positive shift of  $0.54 \text{ cm}^{-1}$ . Comparatively, the next slowest shot, fired at 2.02  $\text{km s}^{-1}$ , showed a larger shift of  $0.63 \text{ cm}^{-1}$ . When the speed was increased to 3.32  $\text{km s}^{-1}$  (Fig. 3a) the amount of the maximum positive shift increased to  $0.91 \text{ cm}^{-1}$  (Fig.

3b). As can be seen in this Figure, Raman shifts were present in varying degrees throughout the crater. The black and dark blue pixels appearing towards the top of the crater in the image are contaminates rather than negative shifts.

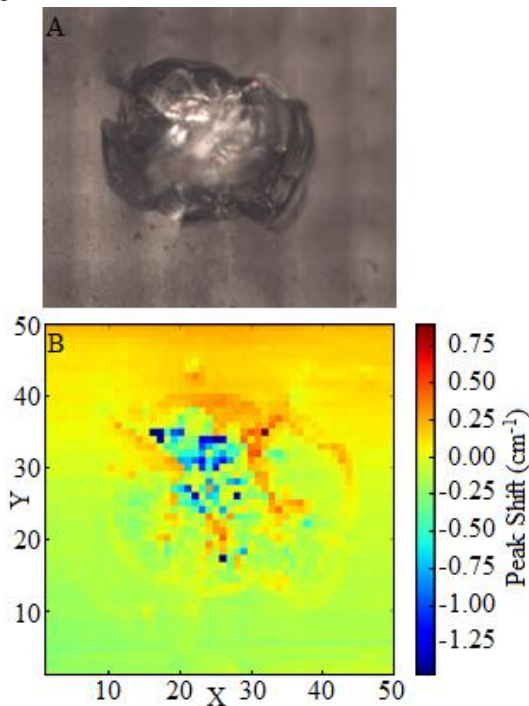


**Fig. 2:** **A)** A microscope image of the ‘bruise’ produced on the surface of the quartz gemstone during the  $0.910 \text{ km s}^{-1}$  impact. **B)** The 2D map showing the shift in the P1 peak position for the ‘bruise’ shown in Fig. 2a.

The fastest shot so far conducted was fired at  $5.27 \text{ km s}^{-1}$  and showed a maximum positive shift of  $1.03 \text{ cm}^{-1}$ . As can be seen by these results, not only does the P1 position shift when the sample is exposed to shock pressure, but there is a positive correlation between the amount of shock pressure the sample is subjected to and the amount by which the P1 position shifts.

**Conclusion:** As can be seen in Table 1, once sufficient velocity has been achieved to generate a crater, the greater the speed of the impact, the greater the maximum positive P1 shift. This is particularly important to keep in mind when reviewing Raman spectra of samples that show evidence of having potentially been subjected to shock pressure. Father research is ongoing to fully understand the correlation between shock pressure and the P1 shift. Additionally, hydro-code modelling is being planned to estimate the shock pressure involved in each impact, as well as obtaining SEM data to confirm the elemental composition of the sample has not changed due to the impact.

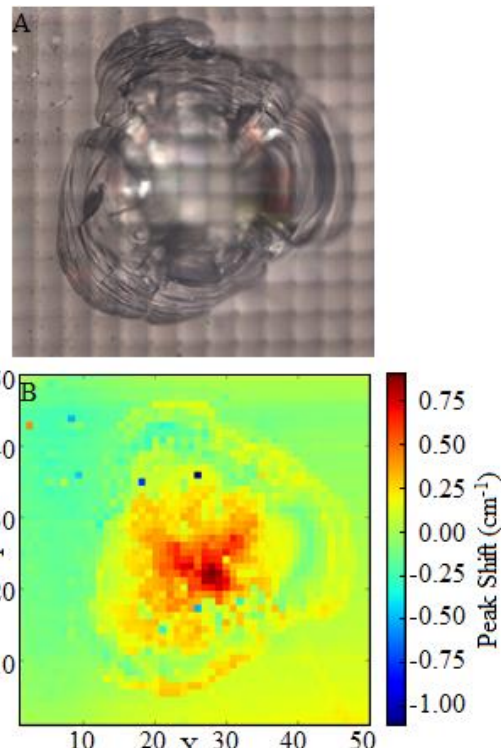


**Fig. 3:** **A)** A microscope image of the crater produced on the surface of the quartz gemstone during the  $3.32 \text{ km s}^{-1}$  impact. **B)** The 2D peak position shift map showing the shift in the P1 peak position for the crater shown in Fig. 3a.

Shot Number	Speed (km s <sup>-1</sup> )	Unshocked P1 Position (cm s <sup>-1</sup> )	Max Shift (cm s <sup>-1</sup> )
S091014#1	0.91	464.20	-1.46
G151014#1	1.35	465.00	0.54
G051114#3	2.02	464.30	0.63
G241014#1	3.32	464.60	0.91
G271114#2	5.27	464.40	1.03

**Table 1:** A table showing the speed, original P1 position and the maximum shift for each shot.

**References:** [1] Bandfield J. L. et al (2004a) *J. Geophys. Res.*, 109, E10009. [2] Rull F. et al. (2011). 42<sup>nd</sup> LPSC abstract #2400. [3] Rull F. et al. (2013). 44<sup>th</sup> LPSC abstract #3110. [4] Wozniakiewicz P. J. et al. (2012). *MAPS*, .47, 4, 660 – 670. [5] Foster N. et al. (2013). *GCA*, 121, 1 – 14. [6] Wozniakiewicz P. J. et al. (2011). *MAPS*, 46, 7, 1007 – 1024. [7] Miljković K. et al. (2013). 44<sup>th</sup> LPSC abstract # 1940. [8] Price M. C. et al. (2013). *Int. J. Astrobiology*, DOI: 10.1017/S1473550413000384. [9] Burchell M. J. et al. (1999). *Meas. Sci. & Tech.*, 10, 41 - 50. [10] Price M. C. et al. *EPSC 2014*, Abstract EPSC2014-91.

**Acknowledgments:** RH thanks the Uni. of Kent for receipt of a PhD. tuition fees scholarship. MCP thanks the STFC, UK.